

Large-area uniform electron doping of graphene by Ag nanofilm ^{EP}

Cite as: AIP Advances **7**, 045209 (2017); <https://doi.org/10.1063/1.4979113>

Submitted: 05 November 2016 . Accepted: 13 March 2017 . Published Online: 12 April 2017

Xiaopeng Guo ^{id}, Lilan Peng, Libin Tang, Jinzhong Xiang, Rongbin Ji, Kai Zhang, Chi Man Luk, Sin Ki Lai, Ruimin Wan, Yu Duan, and Shu Ping Lau ^{id}

COLLECTIONS

^{EP} This paper was selected as an Editor's Pick



View Online



Export Citation



CrossMark

ARTICLES YOU MAY BE INTERESTED IN

[Erbium diffusion in titanium dioxide](#)

AIP Advances **7**, 045202 (2017); <https://doi.org/10.1063/1.4979923>

[Thermal resistance of twist boundaries in silicon nanowires by nonequilibrium molecular dynamics](#)

AIP Advances **7**, 045105 (2017); <https://doi.org/10.1063/1.4979982>

[Functionalization of graphene quantum dots by fluorine: Preparation, properties, application, and their mechanisms](#)

Applied Physics Letters **110**, 221901 (2017); <https://doi.org/10.1063/1.4984238>

AVS Quantum Science

Co-Published by



RECEIVE THE LATEST UPDATES



Large-area uniform electron doping of graphene by Ag nanofilm

Xiaopeng Guo,^{1,2,a} Lilan Peng,^{3,a} Libin Tang,^{2,b} Jinzhong Xiang,^{1,b}
 Rongbin Ji,^{2,b} Kai Zhang,³ Chi Man Luk,⁴ Sin Ki Lai,⁴ Ruimin Wan,²
 Yu Duan,² and Shu Ping Lau⁴

¹*School of Materials Science and Engineering, Yunnan University, Kunming 650091, People's Republic of China*

²*Kunming Institute of Physics, Kunming 650223, People's Republic of China*

³*Chinese Academy of Sciences, Suzhou Institute of Nano-Tech and Nano-Bionics (SINANO), Suzhou 215123, People's Republic of China*

⁴*Department of Applied Physics, The Hong Kong Polytechnic University, Hong Kong, People's Republic of China*

(Received 5 November 2016; accepted 13 March 2017; published online 12 April 2017)

Graphene has attracted much attention at various research fields due to its unique optical, electronic and mechanical properties. Up to now, graphene has not been widely used in optoelectronic fields due to the lack of large-area uniform doped graphene (*n*-doped and *p*-doped) with smooth surface. Therefore, it is rather desired to develop some effective doping methods to extend graphene to optoelectronics. Here we developed a novel doping method to prepare large-area (> centimeter scale) uniform doped graphene film with a nanoscale roughness (RMS roughness ~ 1.4 nm), the method (nano-metal film doping method) is simple but effective. Using this method electron doping (electron-injection) may be easily realized by the simple thermal deposition of Ag nano-film on a transferred CVD graphene. The doping effectiveness has been proved by Raman spectroscopy and spectroscopic ellipsometry. Importantly, our method sheds light on some potential applications of graphene in optoelectronic devices such as photodetectors, LEDs, phototransistors, solar cells, lasers *etc.* © 2017 Author(s). All article content, except where otherwise noted, is licensed under a Creative Commons Attribution (CC BY) license (<http://creativecommons.org/licenses/by/4.0/>). [<http://dx.doi.org/10.1063/1.4979113>]

I. INTRODUCTION

Using graphene as a *p-n* junction in the semiconductor field has been of great interest since the discovery of graphene by K. S. Novoselov *et al.* in 2004.¹ In general, graphene adsorbs oxygen in the air such that pristine graphene is slightly *p*-doped in the air.^{2,3} It is desirable to prepare high quality *n*-doped graphene although the stability and doping quality remain a huge challenge.

Doping methods of graphene are usually classified into three categories: elemental doping, chemical charge induction and metal doping. Elemental doping is generally associated with chemical reaction of chemical compounds with graphene. The elements of the compound form chemical bonding with the carbon atoms. The common doping elements include N,^{4–6} S,^{7,8} I,⁹ B.¹⁰ Co-doping of graphene has been reported with two doping elements at the same time, such as N-S,¹¹ N-B.¹² Elemental doping is usually carried out in-situ during the growth of graphene, or the reduction of graphene oxide using a compound containing the doping elements. Although this method can significantly improve the performance, it inevitably induces undesirable defects

^aThese authors contributed equally to the work

^bCorresponding author: Prof. Libin Tang, E-mail: scitang@163.com. Prof. Jinzhong Xiang E-mail: jzhxiang@ynu.edu.cn. Prof. Rongbin Ji E-mail: jirongbin@gmail.com.

like carbon vacancies and usually involves corrosive or irritating chemical gases or solutions. It is difficult to control the doping amount as well. Chemical charge induction is regarded as surface doping with organic small molecules and polymers. In common practice, the as-grown graphene is firstly transferred to the target substrate. The molecules or polymer solution is then spin-coated on the graphene surface. This approach can preserve the integrity and smoothness of graphene. However, the spin-coating requirement may restrict the large area (in the scale of several or tens of inches), uniform doping of graphene. Examples of materials used for charge induction in graphene are graphitic carbon nitride polymer,^{13,14} aromatic molecules,¹⁵ and conjugated polymers.¹⁶

Metal doping can alter the properties of graphene through the free electrons in metals. The common doping elements are noble metals (Pd, Ru, Rh, Pt, Au, Ag),^{17–21} Al,²² Li,²³ Ca²³ and Ba.²³ Since the metal used for doping is usually in the form of nanoparticles, doping inhomogeneity across the surface of graphene may limit their applications. On the other hand, the doped graphene quantum dots (GQDs) exhibit excellent performance as compared with the doped graphene.²⁴ However, the shortcomings of the doped GQDs such as aggregation and incompatibility with electronic applications due to their nanoscale size are issues that need to be addressed.

Large-area uniform graphene doping method with a nanoscale roughness is rather important for development of optoelectronic devices such as photodetectors, LEDs, phototransistors, solar cells, lasers *etc.* The regular graphene doping methods,²⁵ (TABLE S1 of the [supplementary material](#)) however, seems hard to satisfy the large-area, uniform doping requirements. Therefore, it is rather desired to develop a new graphene doping method to extend graphene's applications to optoelectronics.

In this paper, we develop a novel graphene doping method (nano-metal film doping method) to prepare large-area uniform doped graphene film, the method is simple but effective. The CVD as-grown graphene was doped with silver (Ag) nanofilm deposited by thermal evaporation. The thickness of the film was measured to be ~10 nm by atomic force microscopy (FIG S1 of the [supplementary material](#)). The surface R.M.S. roughness of Ag film was 1.4 nm. The graphene was determined to be monolayer by Raman spectroscopy.^{25,26} This method realizes large-area (not less than 30 inches)²⁷ production of low cost and high quality electron doped graphene, which is compatible with a wide range of industrial applications.

II. EXPERIMENTAL

A. Synthesis of graphene using the CVD method

As illustrated in Figure 1, a piece of copper foil (99.99%, 25 μm thick, MTI) was placed in a vacuum-pumped tube furnace (OTF-1200X, MTI). The tube was evacuated to < 0.2 Pa. Mixture gas (H_2 : Ar = 1: 999.99 vol%, Kunming Pengda gas) was introduced. The temperature in the tube furnace was increased from room temperature to 1000 °C for 0.5 hour under mixture gas flow. Methane (99.999%, Kunming Pengda gas) was introduced at 1000 °C for 10 minutes, and then cooled down to room temperature. All the reagents were used without further purification.

B. Transfer and doping of graphene

The as-grown graphene was spin-coated with poly-methyl methacrylate (PMMA) (M.W. 35000, Ourchem), and the solvent was evaporated at 80 °C. The Cu foil was etched in an aqueous solution of 0.6 mol/L ferric chloride (99.0%, Fengchuan Chem) for over 12 hours. Graphene/PMMA was transferred several times to deionized water before finally transferred onto Si substrate. The PMMA was dissolved in acetone. Ag was deposited on graphene by thermal evaporation. Figure 1(a) shows the schematic diagram of the transfer and doping process of graphene.

C. Characterization

The atomic arrangement was investigated by transmission electron microscope (TEM, Tecnai G2 TF30). The surface morphology and roughness were studied by atomic force microscope (AFM, Bruker Dimension ICON). The Raman spectra were obtained by Renishaw in Via Raman microscope

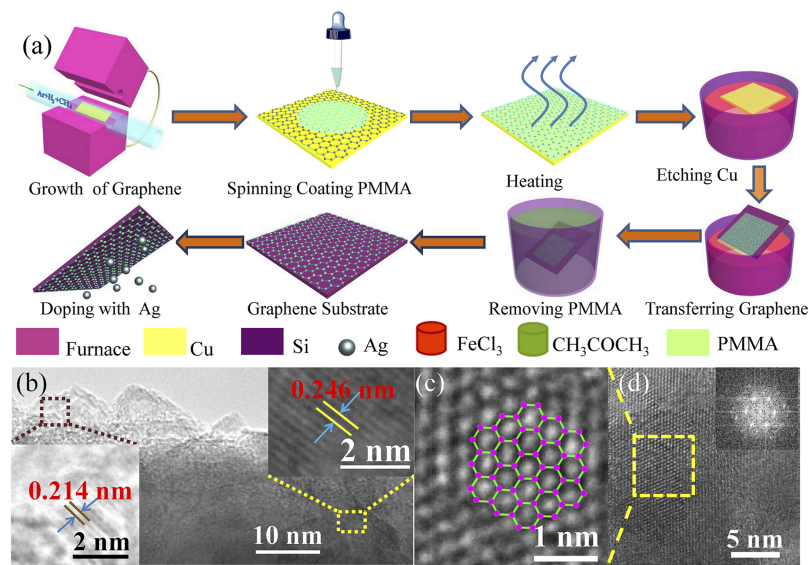


FIG. 1. (a) The schematic illustration for the synthesis and doping of graphene. (b) The TEM images show different sets of lattice planes of graphene. (c) The atomic arrangement of graphene revealed by the high resolution TEM image. (d) High resolution TEM image of graphene. Inset: FFT image of graphene.

with a laser wavelength of 514.5 nm. The ellipsometry spectra were measured using HORIBA Auto SE instrument. The Hall measurements were carried out by Nanometrics HL5500 Hall effect measurement system. The transmission spectra graphene and Ag/graphene were tested using UV-2550 UV-Vis spectrophotometer.

III. RESULTS AND DISCUSSION

Figure 1(b) shows the interplanar spacing for different graphene planes. The insets show the interplanar spacings of 0.214 and 0.246 nm, which corresponds to the (110) and (100) planes of graphene respectively.²⁰ The hexagonal arrangement of carbon atoms can be observed from high resolution TEM images in Figures 1(c). The hexagonal crystal structure of graphene was also confirmed from the fast Fourier transform (FFT) image as shown in the inset of Figure 1(d). The result depicts highly crystalline graphene used in the experiments. Both graphene and Ag/graphene have high transparency (FIG S2 of the [supplementary material](#)).

The Raman spectra of graphene and Ag-doped graphene are shown in Figure 2. Figure 2(a) is the Raman spectrum of pristine graphene. It can be deduced that the graphene is single layer by comparing the G ($\sim 1600\text{ cm}^{-1}$) and 2D ($\sim 2700\text{ cm}^{-1}$) peak intensities, with a 2D/G peak intensity ratio larger than two.²¹ The inset in Figure 2(a) shows a macroscopic comparison of the pristine and Ag-doped graphene under optical microscope, where the Raman spectrum of the pristine and Ag-doped graphene were obtained from graphene deposited on the same Si substrate. In addition, the microscopic images of same area before and after Ag coating is presented in FIG S3 (see [supplementary material](#)). When comparing the Raman spectrum of Ag-doped graphene with the pristine graphene, no significant variation was observed regarding the number of peaks and intensity (Figure 2(b)), especially for the intensity of D peak at $\sim 1350\text{ cm}^{-1}$, which is related to the density of defects in graphene,²⁸ did not become more intense after the deposition of Ag, thus the Ag deposition did not adversely affect the quality of graphene. In addition, from Figures 2(c) and 2(d), both 2D and G peaks show a shift for the Ag-doped graphene. The G peak shifted towards the right by 2.7 cm^{-1} while the 2D peak shifted towards the right by 2.0 cm^{-1} . The full-width-at-half-maximum (FWHM) of the G peak was increased by 1.4 cm^{-1} and that of the 2D peak was decreased by 3.1 cm^{-1} . The Raman peak shifts agree with the Ag doped graphene reported before.²⁹ The differences of the peaks between the doped and pristine graphene were listed at Table I.

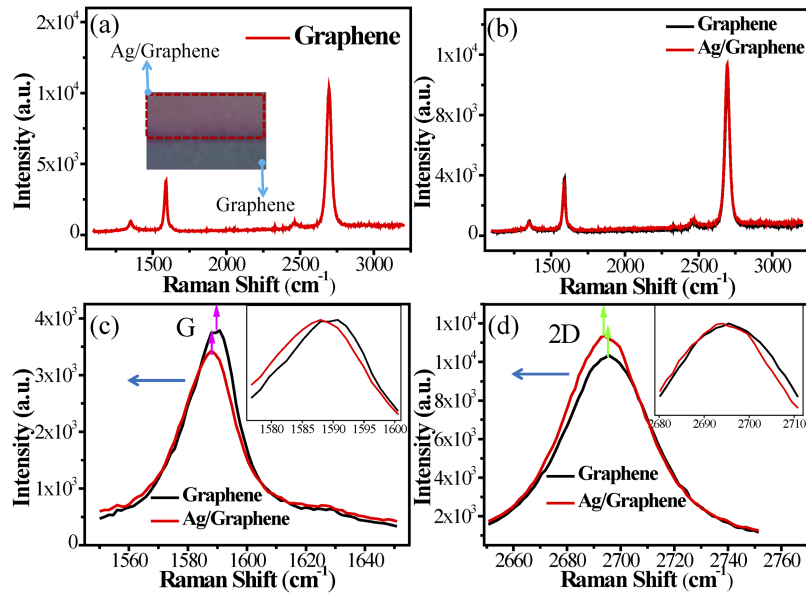


FIG. 2. (a) Raman spectrum of a monolayer graphene used in the experiment. Inset: Optical micrograph of monolayer graphene on Si substrate which was partially doped with Ag. (b) Comparison of Raman spectra of pristine and Ag-doped graphene. The Comparison of the shift of (c) G peaks and (d) 2D peaks between pristine graphene and Ag-doped graphene.

TABLE I. The peak positions and FWHMs of G and 2D Raman peaks for graphene and Ag/graphene.

	G Peak		2D Peak	
	Graphene	Ag/Graphene	Graphene	Ag/Graphene
Position (cm ⁻¹)	1590.6	1587.9	2695.4	2693.4
FWHM (cm ⁻¹)	20.0	21.4	37.1	34.0

Figure 3(a) shows that the surface roughness of the Ag film prepared by thermal deposition was very small (~ 1.4 nm), indicating that it was uniformly doped on the graphene surface. We measured the thickness of Ag nanofilms by AFM, a clear step appeared in the AFM image (FIG S1 of the [supplementary material](#)). Figure 3(b) illustrates the band modulation diagram of graphene due to the Ag-doping effect. Since the single-layer graphene has zero forbidden band,²² the valence and conduction band maximum together with the Fermi level are located at the same energy. The transferred CVD graphene shows a *p*-type conducting because of the oxygen adsorption. When Ag was introduced to graphene, the electron-rich Ag raises the Fermi level of graphene by injecting electrons from Ag to the valence band of graphene, which also explain the increase in the resistivity in Ag-doped graphene (Figure 2(b)) due to a decrease in the carrier concentration at the Fermi level.

The optical properties of graphene and Ag/graphene were studied by spectroscopic ellipsometry (SE). The important wavelength-dependent optical parameters such as reflective index (*n*) and extinction coefficient (*k*) may be calculated from the measured amplitude (*Ψ*) and phase (*Δ*) data through the Kramers-Kronig relations. Figures 3(c)–3(e) are the SE results, which obviously revealed different optical properties between pristine graphene and Ag/graphene, not only in peak positions but also in the intensities. Based on these data, the absorption coefficients (*α*) for graphene and Ag/graphene were derived in Figure 4. Both graphene and Ag/graphene show a very large absorption coefficient ($\alpha > 10^5$ cm⁻¹) for wavelength longer than 500 nm, up to 600 nm, meaning that graphene and Ag/graphene could absorb large amount of light, which imply potentials for high performance solar cells and photodetectors.

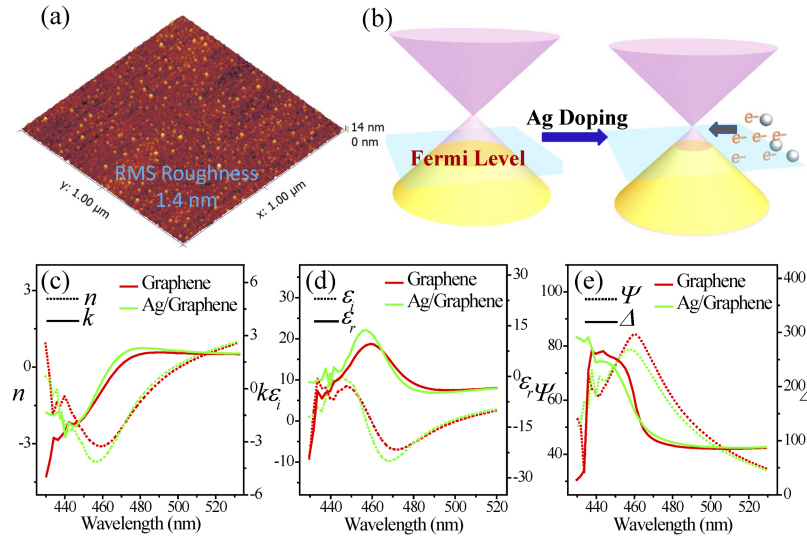


FIG. 3. (a) The AFM image of the thermally deposited Ag film. (b) The schematic illustration of the band modulation of graphene after Ag-doping. (c)-(e) The optical parameters for graphene and Ag/graphene measured by spectroscopic ellipsometry.

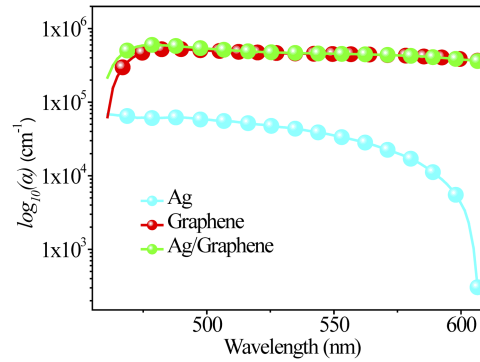


FIG. 4. The logarithmic function of absorption coefficients for Ag, graphene and Ag-doped graphene.

TABLE II. The Hall measurement for graphene and Ag/graphene.

	Resistivity(sheet) Ω/sq	Hall Coef. cm^2/C	Mobility $\text{cm}^2/(\text{V S})$	Concentration(sheet)/ cm^2
Graphene	1458	+79.1	543	$+7.889 \times 10^{12}$
Ag/Graphene	2582	+108	419	$+5.766 \times 10^{12}$

Table II shows the Hall measurements on graphene and Ag/graphene, the results show that hole concentration of graphene has been compensated by electron-injection from Ag nanofilm. Our method provides a technique to tune the properties of graphene by metal nanofilm doping, it can be deduced that the electrical properties (carrier concentration, mobility, conduction type *etc.*) may be adjusted by doping of graphene with nanofilms of different work function metals.

IV. CONCLUSION

In conclusion, we have developed a nano-metal film doping method to adjust graphene's conduction type. Large-area (> centimeter scale) uniform electron doped graphene with a nanoscale

smooth (RMS roughness ~ 1.4 nm) has been obtained by the thermal deposition of Ag nano film on a transferred CVD graphene. The doping method is simple but effective. The Ag-doped graphene also exhibited large absorption coefficient ($\alpha > 10^5$ cm $^{-1}$) at ~ 500 nm, which makes it useful for various applications particularly as potential candidates in the optoelectronics. Our graphene doping method paves the way for graphene based optoelectronic devices such as photodetectors, phototransistors, LEDs, solar cells, lasers *etc.*

SUPPLEMENTARY MATERIAL

See [supplementary material](#) for the thickness of Ag nanofilm measured by AFM (FIG. S1), the transmission spectra of graphene and Ag/graphene and Hall effect device (FIG. S2), the microscopic images of the same area before and after Ag coating (FIG. S3) and the comparison of various methods for the doping of graphene (TABLE S1).

ACKNOWLEDGMENTS

This work was supported by National Natural Science Foundation of China (No. 61106098), and the Key Project of Applied Basic Research of Yunnan Province, China (No. 2012FA003).

- ¹ K. S. Novoselov, A. K. Geim, S. V. Morozov, D. Jiang, Y. Zhang, S. V. Dubonos, I. V. Grigorieva, and A. A. Firsov, *Science* **306**, 666 (2004).
- ² Y. Yang, K. Brenner, and R. Murali, *Carbon* **50**, 1727 (2012).
- ³ S. Rumyantsev, G. Liu, W. Stillman, N. Shur, and A. A. Balandin, *J. Phys.: Condens. Matter* **22**, 395302 (2010).
- ⁴ D. Wei, Y. Liu, Y. Wang, H. Zhang, L. Huang, and G. Yu, *Nano Lett.* **9**, 1752 (2009).
- ⁵ X. R. Wang, X. L. Li, L. Zhang, Y. Yoon, P. K. Weber, H. L. Wang, J. Guo, and H. J. Dai, *Science* **324**, 768 (2009).
- ⁶ H. Wang, T. Maiyalagan, and X. Wang, *ACS Catal.* **2**, 781 (2012).
- ⁷ S. H. Li, Y. C. Li, J. Cao, J. Zhu, L. Z. Fan, and X. H. Li, *Anal. Chem.* **86**, 10201 (2014).
- ⁸ Y. L. Li, J. J. Wang, X. F. Li, D. S. Geng, M. N. Banis, Y. J. Tang, D. N. Wang, R. Y. Li, T.-K. Sham, and X. L. Sun, *J. Mater. Chem.* **22**, 20170 (2012).
- ⁹ Z. Yao, H. G. Nie, Z. Yang, X. M. Zhou, Z. Liu, and S. M. Huang, *Chem. Commun.* **48**, 1027 (2012).
- ¹⁰ Z. S. Wu, W. C. Ren, L. Xu, F. Li, and H. M. Cheng, *ACS Nano* **5**, 5463 (2011).
- ¹¹ Y. Z. Su, Y. Zhang, X. D. Zhuang, S. Li, D. Q. Wu, F. Zhang, and X. L. Feng, *Carbon* **62**, 296 (2013).
- ¹² L. S. Panchakarla, K. S. Subrahmanyam, S. K. Saha, A. Govindaraj, H. R. Krishnamurthy, U. V. Waghmare, and C. N. R. Rao, *Adv. Mater.* **21**, 4726 (2009).
- ¹³ Y. Zhang, T. Mori, L. Niu, and J. Ye, *Energy Environ. Sci.* **4**, 4517 (2011).
- ¹⁴ S. K. Lai, C. Xie, K. S. Teng, Y. Li, F. Tan, F. Yan, and S. P. Lau, *Adv. Optical Mater.* **4**, 555 (2016).
- ¹⁵ X. Dong, D. Fu, W. Fang, Y. Shi, P. Chen, and L.-J. Li, *Small* **5**, 1422 (2009).
- ¹⁶ Y. Gao, H. L. Yip, K. S. Chen, K. M. O'Malley, O. Acton, Y. Sun, and A. K. Y. Jen, *Adv. Mater.* **23**, 1903 (2011).
- ¹⁷ J. Lee, K. S. Novoselov, and H. S. Shin, *ACS Nano* **5**, 608 (2011).
- ¹⁸ Z. K. Liu, J. H. Li, Z. H. Sun, G. A. Tai, S. P. Lau, and F. Yan, *ACS Nano* **6**, 810 (2012).
- ¹⁹ M. Giovanni, H. L. Poh, A. Ambrosi, G. Zhao, Z. Sofer, F. Sanek, B. Khezri, R. D. Webster, and M. Pumera, *Nanoscale* **4**, 5002 (2012).
- ²⁰ S. K. Lai, C. M. Luk, L. Tang, K. S. Teng, and S. P. Lau, *Nanoscale* **7**, 5338 (2015).
- ²¹ G. Giovannetti, P. A. Khomyakov, G. Brocks, V. M. Karpan, J. Van Den Brink, and P. J. Kelly, *Phys. Rev. Lett.* **101**, 026803 (2008).
- ²² J. Dai, J. Yuan, and P. Giannozzi, *Appl. Phys. Lett.* **95**, 232105 (2009).
- ²³ J. Pešić, V. Damjanović, R. Gajić, K. Hingerl, and M. Belić, *EPL* **112**, 67006 (2015).
- ²⁴ J. H. Zhao, L. B. Tang, J. Z. Xiang, R. B. Ji, Y. B. Hu, J. Yuan, J. Zhao, Y. J. Tai, and Y. H. Cai, *RSC Adv.* **5**, 29222 (2015).
- ²⁵ A. C. Ferrari, J. C. Meyer, V. Scardaci, C. Casiraghi, M. Lazzeri, F. Mauri, S. Piscanec, D. Jiang, K. S. Novoselov, S. Roth, and A. K. Geim, *Phys. Rev. Lett.* **97**, 187401 (2006).
- ²⁶ S. Pisana, M. Lazzeri, C. Casiraghi, K. S. Novoselov, A. K. Geim, A. C. Ferrari, and F. Mauri, *Nat. Mater.* **6**, 198 (2007).
- ²⁷ S. Bae, H. Kim, Y. Lee, X. Xu, J.-S. Park, Y. Zheng, J. Balakrishnan, T. Lei, H. R. Kim, Y. I. Song, Y.-J. Kim, K. S. Kim, B. Özyilmaz, J.-H. Ahn, B. H. Hong, and S. Iijima, *Nat. Nanotechnol.* **5**, 574 (2010).
- ²⁸ S. K. Lai, L. Tang, Y. Y. Hui, C. M. Luk, and S. P. Lau, *J. Mater. Chem. C* **2**, 6971 (2014).
- ²⁹ F. Jimenez-Villacorta, E. Climent-Pascual, R. Ramirez-Jimenez, J. Sanchez-Marcos, C. Prieto, and A. de Andrés, *Carbon* **101**, 305 (2016).